IOSR Journal of Electronics and Communication Engineering (IOSR-JECE)
e-ISSN: 2278-2834,p- ISSN: 2278-8735. Volume 5, Issue 6 (Mar. - Apr. 2013), PP 97-105
www.iosrjournals.org

Designing and Performance Evaluation of 64 QAM OFDM System

Sahasha Namdeo[1], Reena Rani[2]
[1](M.Tech, Electronics and Communication, Maharshi Dayanand University, Rohtak, Haryana India)
[2](M.Tech, Electronics and Communication, Maharshi Dayanand University, Rohtak, Haryana India)

Abstract (11Bold) : *— In this report, the performance analysis of 64 QAM-OFDM wireless communication systems affected by AWGN in terms of Symbol Error Rate and Throughput is addressed. 64 QAM (64 ary Quadrature Amplitude Modulation) is the one of the effective digital modulation technique as it is more power efficient for larger values of M(64). The MATLAB script based model of the 64 QAM-OFDM system with normal AWGN channel and Rayleigh fading channel has been made for study error performance and throughput under different channel conditions. This simulated model maximizes the system throughput in the presence of narrowband interference, while guaranteeing a SER below a predefined threshold. The SER calculation is accomplished by means of modelling the decision variable at the receiver as a particular case of quadratic form D in complex Gaussian random variables. Lastly comparative study of SER performance of 64 QAM-OFDM simulated & 64 QAM-OFDM theoretical under AWGN channel has been given. Also performance of the system is given in terms of throughput (received bits/ofm symbol) is given in a plot for different SNR.*

Keywords (11Bold) *–64 QAM, BPSK, OFDM, PDF, SNR.*

I. INTRODUCTION

1.1 Orthogonal Frequency Division Multiplexing

In OFDM systems, the available bandwidth is broken into many narrower subcarriers and the data is divided into parallel streams, one for each subcarrier each of which is then modulated using varying levels of QAM modulation e.g. QPSK, 16QAM, 64QAM or higher orders as required by the desired signal quality. The linear combination of the instantaneous signals on each of the subcarriers constitutes the OFDM symbols. The spectrum of OFDM is depicted in fig.1.1. Each of the OFDM symbol is preceded by a cyclic prefix (CP) which is effectively used to eliminate Intersymbol Interference (ISI) and the subcarriers are also very tightly spaced for efficient utilization of the available bandwidth [1].

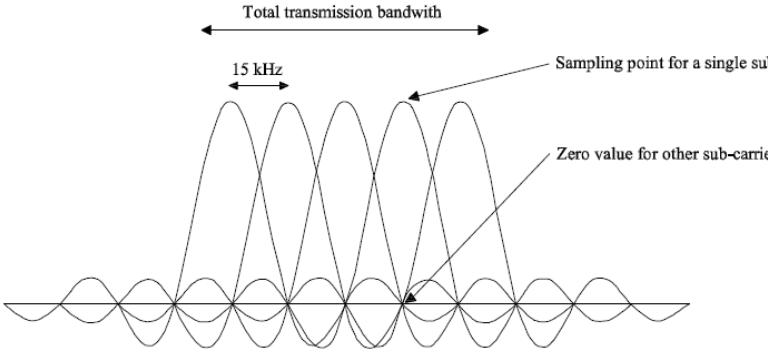

Figure 1.1 OFDM Spectrum

OFDM provides an effective method to mitigate intersymbol interference (ISI) in wideband signalling over multipath radio channels. The main idea is to send the data in parallel over a number of narrowband flat subchannels (see Fig. 1.2). This is efficiently achieved by using a set of overlapped orthogonal signals to partition the channel. A transceiver can be realized using a number of coherent QAM modems which are equally spaced in the frequency domain and which can be implemented using the IDFT on the transmitter end and the DFT on the receiving end [6,7]. Due to the fact that the intercarrier spacing in OFDM is relatively small, OFDM transceivers are somewhat more sensitive to phase noise by comparison to single carrier transceivers. It is the purpose of this paper to examine the impact of L.O. phase noise on the BER performance of OFDM signals over both AWGN and frequency selective channels. The paper first discusses the relationship between the continuous time, continuous frequency L.O. phase noise model and the discrete time, discrete frequency process that is seen by the OFDM system. An analysis of the OFDM receiver is presented to assess

the impact of the phase noise on the decision variables at the receiver (which are the received signal samples corrupted by noise, just before making hard decisions regarding the received data). It is then shown that the effect of phase noise on the decision variables is composed of two components: a common component which affects all data symbols equally and as such causes a sometimes visible rotation of the signal constellation, and a second component which is more like Gaussian noise and thus affects the received data points in a somewhat random manner. This representation in terms of common and foreign components has been pointed out in the literature [8]–[10]. What we introduce here that is different, is that the temporal variations of the rotational component and its dependence on the frequency spacing between the system carriers play an important role in determining the symbol-error rate performance of the OFDM system, particularly at higher operating SNR conditions. Taking the temporal variations of the rotational component of the phase noises into account, we then proceeded to derive analytical expressions for the average probability of error for 64-QAM OFDM. The resulting formulas are in a closed form which includes several integrals over the Gaussian probability curve. The analytical results are then used to quantify the impact of certain phase noise masks on the average BER performance under different SNR conditions and also subject to variations of the OFDM frame length. Computer simulation is used to treat the problem over channels with arbitrary multipath profiles and also, to investigate the impact of phase noise on channel estimation and channel equalization. The simulation model requires a user specified phase noise mask as an input. It also requires the user to identify system parameters such as sampling frequency, OFDM frame length and the size of the signal constellation.

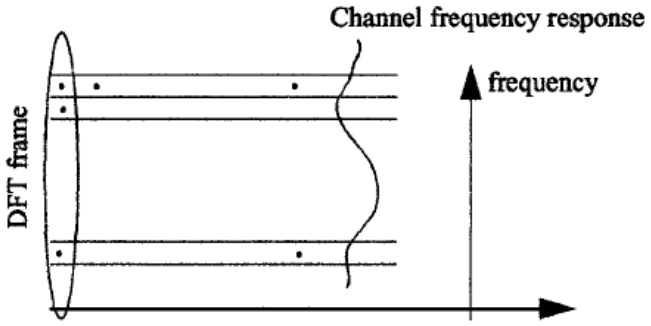

Figure 1.2 Using OFDM to mitigate ISI

1.2. System Description and Model

A functional block diagram of an OFDM system is shown in Fig. 1.3. The incoming data is fist applied to a baseband M-ary QAM modulator which maps each L= log2M binary bits into one of the M constellation points. The M-QAM points coming out of the baseband modulator are then grouped into frames, each containing N complex constellation points. Each frame is applied to an inverse DFT processor which outputs N-complex transform coefficients. A circular prefix of length Np is then appended to the N complex transform coefficients to form a transmitted frame which is N + Np points long. The transmitted frame is then applied to a serial-to-parallel converter and then applied to an IQ modulator to translate the spectral content of the signal to some UHF or microwave frequency band. The IQ modulation is accomplished by multiplying the complex envelope of the signal with the output of a local oscillator. This step is often accomplished at a convenient IF frequency and the modulated signal is then upconverted using a higher frequency local oscillator. For our purpose, it is sufficient to consider one local oscillator as indicated in, Fig. 1.3. The local oscillator is not perfect. Its output is usually degraded due to many factors, including short term frequency drift that may in part be caused by temperature variations. The short term frequency drifts manifest themselves as phase noise which has traditionally been characterized in terms of its power spectral density.

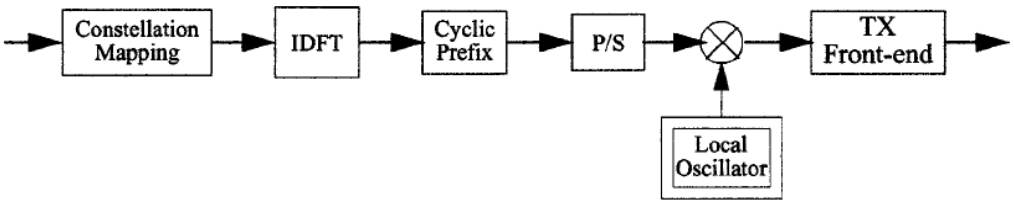

Figure 1.3 Block diagram of an OFDM transmitter.

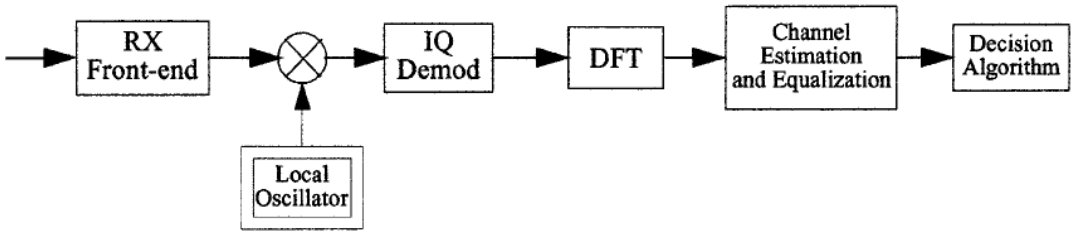

Figure 1.4 Block diagram of an OFDM receiver.

A functional block diagram of a simplified OFDM receiver is depicted in Fig. 1.4. The received signal, usually corrupted by additive noise and channel distortion, is first applied to a low noise microwave front-end where it is amplified and perhaps filtered to suppress unwanted interference. The received signal is then downconverted to an IF frequency and applied to an I&Q demodulator which brings the signal down to baseband in the form in-phase and quadrature components. These in turn are applied to a A/D converter which outputs complex baseband samples at a rate of one sample per received symbol. The complex samples are then grouped into received frames which contain N + Np points each. Assuming that the frame synchronization is working, the received frames are first reduced to N points each by removing the circular prefix, and then are applied to an N -point DFT processor. The received frame is also used to estimate the frequency response of the channel. The DFT output is then equalized to generate -decision variables which may be used to recover the data either based on threshold comparison or applied to a sequential estimation procedure such as the Viterbi algorithm.The important block in Fig. 1.4 is the local oscillator, which like the transmitter local oscillator may have its own phase noise which will degrade the quality of the received signal and the overall BER performance. For analog TV (ATV) applications the Tx local oscillator is of much better spectral purity since this exists only in the base station and as such it does not have to be very economical. The Rx local oscillator signal on the other hand is provided with a cheap commercial TV tuner which exhibits high levels of phase noise. It is for this reason that we will concentrate on the Rx LO phase noise without explicit mention of the Tx LO phase noise. It should however be mentioned that the analysis we will develop can still be applied to cases where the phase noise is introduced by a combination of both local oscillators.

1.3. M-QAM constellation

The number of points in the constellation is defined as, $M = 2^b$ where b is the number of bits in each constellation symbol. In this analysis, it is desirable to restrict b to be an even number for the following reasons :

1. Half the bits are represented on the real axis and half the bits are represented on imaginary axis. The in-phase and quadrature signals are independent $b/2$ level Pulse Amplitude Modulation (PAM) signals. This simplifies the design of mapper.
2. For decoding, symbol decisions may be applied independently on the real and imaginary axis, simplifying the receiver implementation.

Note that the above square constellation is not the most optimal scheme for a given signal to noise ratio.

1.3.1. Average energy of an M-QAM constellation

In a general M-QAM constellation where $M = 2^b$ and b the number of bits in each constellation is even, the alphabets used are:

$$\alpha_{MQAM} = \{\pm(2m-1) \pm (2m-1)j\}, \text{ where } m \in \left\{1, \cdots, \frac{\sqrt{M}}{2}\right\}. \quad (1)$$

For example, considering a 64-QAM ($M = 64$) constellation, $m \in \{1, 2, 3, 4\}$ and the alphabets are:

$$\alpha_{64\ QAM} = \begin{matrix} \pm 7 \pm 7j & \pm 7 \pm 5j & \pm 7 \pm 3j & \pm 7 \pm 1j \\ \pm 5 \pm 7j & \pm 5 \pm 5j & \pm 5 \pm 3j & \pm 5 \pm 1j \\ \pm 3 \pm 7j & \pm 3 \pm 5j & \pm 3 \pm 3j & \pm 3 \pm 1j \\ \pm 1 \pm 7j & \pm 1 \pm 5j & \pm 1 \pm 3j & \pm 1 \pm 1j \end{matrix}$$

For computing the average energy of the M-QAM constellation, let us proceed as follows:

(a) Find the sum of energy of the individual alphabets:

$$E_\alpha = \sum_{m=1}^{\frac{\sqrt{M}}{2}} \left|(2m-1)+j(2m-1)\right|^2 = \frac{\sqrt{M}}{3}(M-1) \quad (2)$$

(b) Each alphabet is used $2\sqrt{M}$ times in the M-QAM constellation.

(c) So, to find the average energy from M constellation symbols, divide the product of (a) and (b) by M.

Plugging in the number for 64-QAM:

$$E_{64QAM} = \frac{2}{3}(64-1) = 42.$$

Plugging in the number for 16-QAM:

$$E_{16QAM} = \frac{2}{3}(16-1) = 10.$$

From the above explanations, it is reasonably intuitive to guess that the scaling factor of $\frac{1}{\sqrt{10}}, \frac{1}{\sqrt{42}}$ which is seen along with 16-QAM, 64-QAM constellations respectively is for normalizing the average transmit power to unity.

1.3.2. Types of constellation points in M-QAM

There are three types of constellation points in a general M-QAM constellation:

(a) Constellation points in the corner (red-square)

The number of constellation points in the corner in any M-QAM constellation is always 4, i.e

$$N_{corner} = 4$$

(b) Constellation points in the inside (magneta-diamond)

The number of constellation points inside is,

$$N_{inside} = (\sqrt{M}-2)(\sqrt{M}-2). \quad (3)$$

For example with M=64, there are 36 constellation points in the inside.

(c) Constellation points neither at the corner, nor at the center (blue-star) The number of constellation points of this category is:

$$N_{\text{neither inside nor corner}} = 4(\sqrt{M}-2). \quad (4)$$

For example with M=64, there are 24 constellation points in the inside.

1.4. Additive White Gaussian Noise (AWGN) channel

Let the received symbol is,

$y = k\sqrt{E_s}s+n$, where

E_s is the energy,

$k = \sqrt{\frac{1}{\frac{2}{3}(M-1)}}$ is the normalizing factor,

s is the transmit symbol and

n is the noise.

Assume that the additive noise n follows the Gaussian probability distribution function,

$$p(x) = \frac{1}{\sqrt{2\pi\sigma^2}} e^{\frac{-(x-\mu)^2}{2\sigma^2}} \quad (5)$$

With mean $\mu = 0$ and variance $\sigma^2 = \frac{N_0}{2}$.

Symbol in the inside $I = +1, Q = +1$ (magenta-diamond)

The conditional probability distribution function (PDF) of y given that the transmitted symbol is $\left\{+k\sqrt{E_s}, +k\sqrt{E_s}\right\}$:

$$p(y|inside) = \frac{1}{\sqrt{\pi N_0}} e^{\frac{-(y-k\sqrt{Es})^2}{N_0}}. \quad (6)$$

As can be seen from the above figure, the symbol in the inside is decoded correctly only if real part of y $(\Re y)$ lies in between 0 to 2 and the imaginary part of y $(\Im y)$ lies in between 0 to 2. The probability of

correct demodulation is,

$$p(c|inside) = p\left(\Re y>0, \Re y \le 2k\sqrt{E_s}|+1\right)p\left(\Im y>0, \Im y \le 2k\sqrt{E_s}|+1\right) \quad (7)$$

The probability of the real component falling within 0 to 2 can be found by integrating the probability distribution function of two parts:

(a) Find the probability that the real component lies from 2 to $+\infty$.

(b) Find the probability that the real component lies from $-\infty$ to 0.

(c) Given that the total probability is always 1, for finding the probability of the real component lies between 0 to 2, subtract the sum of (a) and (b) from 1.

$$erfc(x) = \frac{2}{\sqrt{\pi}}\int_{x}^{\infty} e^{-x^2}dx$$

Note: The complementary error function, . (8)

Similarly,

$$p\left(\Im y>0, \Im y \le 2k\sqrt{E_s}|+1\right) = 1-erfc\left(k\sqrt{\frac{E_s}{N_0}}\right). \quad (9)$$

From the above equations,

$$p(c|inside) = \left[1-erfc\left(\sqrt{\frac{E_s}{10N_o}}\right)\right]\left[1-erfc\left(\sqrt{\frac{E_s}{10N_o}}\right)\right]. \quad (10)$$

The probability of the symbol decoded being in error is as follow.

.

Symbol in the corner $I=+7, Q=+7$ **(red-square)**

The conditional probability distribution function (PDF) of y given that the transmitted symbol is $\left\{+7k\sqrt{E_s}, +7k\sqrt{E_s}\right\}$:

$$p(y|inside) = \frac{1}{\sqrt{\pi N_0}}e^{\frac{-(y-7k\sqrt{Es})^2}{N_0}} \quad . \quad (11)$$

As can be seen from the above figure, the symbol in the inside is decoded correctly only if real part of y $(\Re y)$ lies from 6 to ∞ and the imaginary part of y $(\Im y)$ lies from 6 to ∞.

$$p(c|corner) = p\left(\Re y>6, \Re y \le \infty|+7\right)p\left(\Im y>0, \Im y \le \infty|+7\right) \quad (12)$$

For finding the probability that the real component lies from 6 to ∞, one can integrate the probability distribution function of the received symbol.

$$p\left(\Re y>6, \Re y \le \infty|+7\right) = \frac{1}{\sqrt{\pi N_0}}\int_{6k\sqrt{E_s}}^{+\infty} e^{\frac{-(y-7k\sqrt{Es})^2}{N_0}}dy$$

$$= 1-\frac{1}{2}erfc\left(k\sqrt{\frac{E_s}{N_0}}\right) \quad (13)$$

Similarly,

$$p\left(\Im y>6, \Im y \le \infty|+7\right) = \frac{1}{\sqrt{\pi N_0}}\int_{6k\sqrt{E_s}}^{+\infty} e^{\frac{-(y-7k\sqrt{Es})^2}{N_0}}dy$$

$$= 1-\frac{1}{2}erfc\left(k\sqrt{\frac{E_s}{N_0}}\right) \quad (14)$$

.

So, probability that the decoded symbol is correct given $I=+7, Q=+7$ is transmitted is,

$$p(c|corner) = \left[1-\tfrac{1}{2}erfc\left(k\sqrt{\frac{E_s}{N_0}}\right)\right]\left[1-\tfrac{1}{2}erfc\left(k\sqrt{\frac{E_s}{N_0}}\right)\right]$$
$$= 1-erfc\left(k\sqrt{\frac{E_s}{N_0}}\right)+\tfrac{1}{4}erfc^2\left(k\sqrt{\frac{E_s}{N_0}}\right)$$

. (15)

Now, the probability of the symbol decoded being in error is,

$$p(e|corner) = 1-p(c|corner)$$
$$= erfc\left(k\sqrt{\frac{E_s}{N_0}}\right)-\tfrac{1}{4}erfc^2\left(k\sqrt{\frac{E_s}{N_0}}\right)$$

. (16)

Symbol neither at the corner nor inside $I=+7,Q=+1$ **(blue-star)**

As can be seen from the above figure, the symbol in the inside is decoded correctly only if real part of y $(\Re y)$ lies from 6 to ∞ and the imaginary part of y $(\Im y)$ lies from 0 to 2.

$$p(c|corner) = p\left(\Re y>6,\Re y\le\infty|+7\right)p\left(\Im y>0,\Im y\le\infty|+7\right) \quad (17)$$

For finding the probability that the real component lies from 6 to ∞, one can integrate the probability distribution function of the received symbol.

$$p\left(\Re y>6,\Re y\le\infty|+7\right) = \frac{1}{\sqrt{\pi N_0}}\int_{6k\sqrt{E_s}}^{+\infty} e^{\frac{-(y-7k\sqrt{E_s})^2}{N_0}}dy$$
$$= 1-\tfrac{1}{2}erfc\left(k\sqrt{\frac{E_s}{N_0}}\right)$$

. (18)

As described for the symbol in the inside scenario, the probability of the imaginary component falling with in 0 to 2 can be found by integrating the probability distribution function of two parts:

(a) Find the probability that the imaginary component lies from 2 to $+\infty$.

(b) Find the probability that the imaginary component lies from $-\infty$ to 0.

(c) As the total probability is 1, for finding the probability of the imaginary component lies within 0 to 2, subtract the sum of (a) and (b) from 1.

$$p\left(\Im y>0,\Im y\le 2k\sqrt{E_s}|+1\right) = 1-\left[\frac{1}{\sqrt{\pi N_0}}\int_{-\infty}^{0} e^{\frac{-(y-k\sqrt{E_s})^2}{N_0}}dy+\frac{1}{\sqrt{\pi N_0}}\int_{2k\sqrt{E_s}}^{+\infty} e^{\frac{-(y-k\sqrt{E_s})^2}{N_0}}dy\right]$$
$$= 1-erfc\left(k\sqrt{\frac{E_s}{N_0}}\right)$$

(19)

So the probability that the symbol is decoded correctly technologies. The analytical performance of most of wireless communication systems under different fading conditions has already been accomplished when perfect channel state information (CSI) is assumed to be known at the receiver side (or even at the transmitter side, if required) [5, 6]. These results hence are useful to determine the maximum achievable performance of these systems under ideal conditions. However, in practice there exist many factors which may limit their performance: the appearance of interfering signals, the consideration of imperfect CSI, or non-idealities due to physical implementation such as carrier frequency offset (CFO), in-phase/quadrature (I/Q) imbalance and direct-current (DC) offsets are valid examples. is,

$$p(c|\text{neither inside nor corner}) = \left[1-erfc\left(k\sqrt{\frac{E_s}{N_0}}\right)\right]\left[1-\frac{1}{2}erfc\left(k\sqrt{\frac{E_s}{N_0}}\right)\right]$$
$$= 1-\frac{3}{2}erfc\left(k\sqrt{\frac{E_s}{N_0}}\right)+\frac{1}{2}erfc^2\left(k\sqrt{\frac{E_s}{N_0}}\right)$$

(20)

The probability of error is,

$$p(e|\text{neither inside nor corner}) = 1-p(c|\text{neither inside nor corner})$$
$$= \frac{3}{2}erfc\left(k\sqrt{\frac{E_s}{N_0}}\right)-\frac{1}{2}erfc^2\left(k\sqrt{\frac{E_s}{N_0}}\right)$$

(21)

1.5. Total symbol error probability

Given that we have computed the individual symbol error probability for each of the three types of constellation points, to find the joint symbol error rate we compute the average error i.e.

$$P(e|MQAM) = \frac{\begin{array}{l}N_{inside}p(e|inside)+\\ N_{corner}p(e|corner)+\\ N_{\text{neither inside nor corner}}p(e|\text{neither inside nor corner})\end{array}}{M}$$

(22)

Pluging in the equations,

$$P(e|MQAM) = 2\left(1-\frac{1}{\sqrt{M}}\right)erfc\left(k\sqrt{\frac{E_s}{N_0}}\right)-\left(1-\frac{2}{\sqrt{M}}+\frac{1}{M}\right)erfc^2\left(k\sqrt{\frac{E_s}{N_0}}\right)$$

(23)

The measurement of the performance in communication systems has always been a matter of extreme interest since their very origin [1–3]. Besides the channel capacity, which basically provides information about the limiting error-free information rate that can be achieved, this performance is usually quantified in terms of the Symbol Error Rate (SER) or the Bit Error Rate (BER). Depending on the characteristics of the channel fading and the modulation scheme, the performance analysis can be conducted following different approaches. One of the milestone reference works in this area was published by Simon and Alouini [4], where the performance of a number of digital communication systems under different fading conditions was analyzed following a common strategy. Most of the results provided in this paper allows obtaining the SER in exact closed-form, whereas in other cases a numerical integration was necessary. The appearance of new digital communication systems that employ new modulation or transmission schemes leads to the necessity of evaluating their performance in order to enable a fair comparison with the existing techniques. Some examples are the use of multiple antennas, usually referred to as multiple-input multiple-output (MIMO) systems, or the orthogonal frequency division multiplexing (OFDM) technique. Both MIMO and OFDM have been incorporated in many commercial and under-development wireless communication

II. METHODOLOGY

2.1. *64 QAM*

1. Use OFDM Specifications like FFT Size, Number of Data Subcarriers,Number of Bits Per OFDM Symbol (Same as the Number of Subcarriers for BPSK), Number of OFDM Symbols
2. Find Out Modulation & Average Energy of 64-QAM
3. Find out SNR according to the accounting for the used subcarriers and cyclic prefix.
4. Find out Transmitter Input
5. Now Calculate Gaussian Noise of Unit Variance, 0 Mean
6. Add Noise to the Transmitter Input

7. Formatting the Received Vector into Symbols and Converting to Frequency Domain
8. Apply Demodulation and Converting to Vector
9. Counting the Errors by Subtracting output Demodulated Vector on receiving side from the Transmitter input.

III. RESULTS AND DISCUSSIONS

3.1. COMPARATIVE BER PERFORMANCE OF M-ARY QAM-OFDM.

The Bit Error Rate (BER) performance against signal to noise ratio (Eb/No) of 64QAM-OFDM & 128QAM-OFDM in both AWGN channel & multipath fading channel has been shown in figure 4 & figure 5 respectively. The BER decreases sharply with the increase in the signal to noise ratio in both AWGN channel & multipath fading channel but the bit error rate in multipath fading channel is higher than normal AWGN channel.

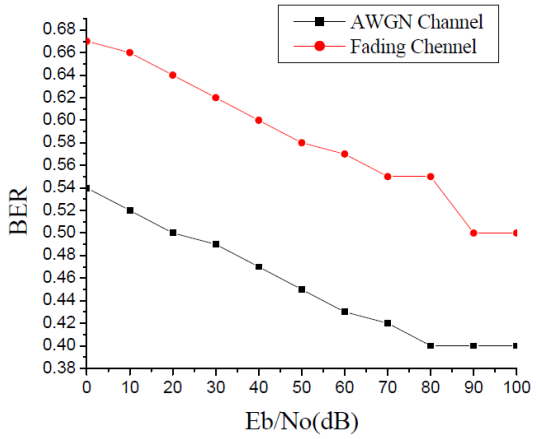

Figure 3.1: E_b/N_0 vs. BER for 64QAM-OFDM system in AWGN channel & Multipath fading channel [12]

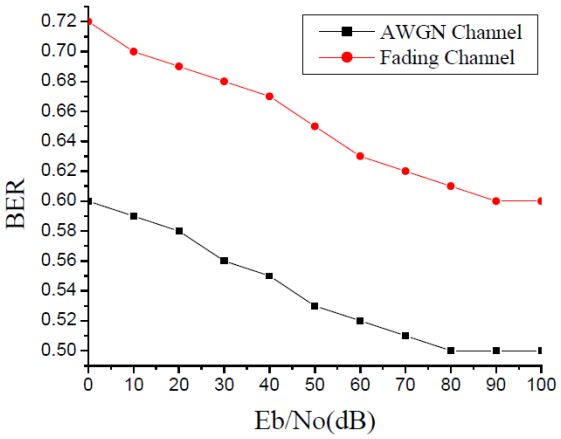

Figure3.2: E_b/N_0 vs. BER for 128QAM-OFDM system in AWGN channel & Multipath fading channel [12]

IV. CONCLUSION

In this document, an algorithm is designed to maximize the OFDM system throughput in the presence of AWGN imperfect channel estimation. The average throughput of the OFDM system is maximized under the constraint of a BER below a target value. As expected, the average throughput increases as the SIR increase, respectively. Moreover, increasing the channel estimation error variance reduces the average throughput. In future work, we will extend the proposed algorithm to include power loading, and impose a constraint on the maximum transmit power to reduce the OFDM cognitive user spectrum leakage, in addition to considering spectrum sculpting techniques.

REFERENCES

Journal Papers:

[1] Pussadee Kiratipongvooth, "Bit Error Probability of Cooperative Diversity for M-ary QAM OFDM-based system with Best Relay Selection" , *International Conference on Information and Electronics Engineering 2011IPCSIT vol.6 (2011) © (2011) IACSIT Press, Singapore*

[2] Abhijyoti Ghosh, "Comparative BER Performance of M-ary QAM-OFDM System in AWGN & Multipath Fading Channel", International Journal on Computer Science and Engineering (IJCSE), Vol. 4 No. 06 June 2012

[3] Ebrahim Bedeer, "Adaptive Bit Allocation for OFDM Cognitive Radio Systems with Imperfect Channel Estimation", 2012 IEEE

[4] Mitalee Agrawal , "BER Analysis of MIMO OFDM System for AWGN & Rayleigh Fading Channel" , *International Journal of Computer Applications (0975 – 8887) Volume 34– No.9, November 2011*

[5] M. Di Renzo, F. Graziosi, and F. Santucci, "On the cumulative distribution function of quadratic-form receivers over generalized fading channels with tone interference," *Communications, IEEE Transactions on*, vol. 57, pp. 2122 –2137, jul. 2009.

[6] F. J. Lopez-Martinez, E. Martos-Naya, J. F. Paris, and A. J. Goldsmith, "BER Analysis for MIMO-OFDM Beamforming with MRC under Channel Prediction and Interpolation Errors," in *Proc. IEEE Global Telecommunications Conf. GLOBECOM 2009*, pp. 1–7, 2009.

[7] F. J. Lopez-Martinez, E. Martos-Naya, J. F. Paris, and U. Fernandez-Plazaola, "Generalized BER Analysis of QAM and its Application to MRC under Imperfect CSI and Interference in Ricean Fading Channels," *IEEE Transactions on Vehicular Technology*, vol. 59, pp. 2598–2604, June 2010.

[8] F. J. Lopez-Martinez, E. Martos-Naya, J. F. Paris, and J. T. Entrambasaguas, "BER analysis of direct conversion OFDM systems with MRC under channel estimation errors," *IEEE Communications Letters*, vol. 14, pp. 423–425, May 2010.

[9] F. J. Lopez-Martinez, E. Martos-Naya, K. K. Wong, and J. Entrambasaguas, "Closed- Form BER Analysis of Alamouti-MRC Systems with ICSI in Ricean Fading Channels," *IEEE Communications Letters*, vol. 1, no. Accepted for publication, pp. 1–3, 2011.

[10] F. J. Lopez-Martinez, E. Martos-Naya, J. F. Paris, and J. Entrambasaguas, "Exact Closed-Form BER Analysis of OFDM Systems in the presence of IQ imbalances and ICSI," *IEEE Transactions on Wireless Communications*, vol. 1, no. 2nd round of reviews, pp. 1–7, 2011.

[11] M. Inamori, A. Bostamam, Y. Sanada, and H. Minami, "IQ imbalance compensation scheme in the presence of frequency offset and dynamic DC offset for a direct conversion receiver," *IEEE Transactions on Wireless Communications*, vol. 8, pp. 2214 –2220, may 2009.

[12] Y. Yoshida, K. Hayashi, H. Sakai, and W. Bocquet, "Analysis and Compensation of Transmitter IQ Imbalances in OFDMA and SC-FDMA Systems," IEEE Transactions on Signal Processing, vol. 57, pp. 3119 –3129, aug. 2009.

[13] Q. Zou, A. Tarighat, and A. Sayed, "Joint compensation of IQ imbalance and phase noise in OFDM wireless systems," *IEEE Transactions on Communications*, vol. 57, pp. 404 –414, february 2009.

[14] H. Minn and D. Munoz, "Pilot Designs for Channel Estimation of OFDM Systems with Frequency-Dependent I/Q Imbalances," in *IEEE Wireless Communications and Networking Conference, 2009. WCNC 2009.*, pp. 1 –6, april 2009.